

# Clinical applications of deep learning in distinguishing benign from malignant pulmonary nodules in computed tomography scans

Yongzhong Xu\*, Yunxin Li, Feng Wang, Yafei Zhang, Delong Huang

Imaging Department, Yantaishan Hospital, Yantai, Shandong, China

**Submitted:** 9 October 2024; **Accepted:** 11 March 2025

**Online publication:** 18 May 2025

Arch Med Sci 2026; 22 (1): 12–26

DOI: <https://doi.org/10.5114/aoms/202835>

Copyright © 2025 Termedia & Banach

**\*Corresponding author:**

Yongzhong Xu

Imaging Department

Yantaishan Hospital

Yantai, Shandong

264003, China

E-mail: [13220931662@163.com](mailto:13220931662@163.com)

com

## Abstract

Early diagnosis is crucial for improving the prognosis of lung cancer, one of the leading causes of cancer-related deaths. Lung cancer includes small cell lung cancer (SCLC, ~15% of cases) and non-small cell lung cancer (NSCLC, ~80–85%). Prognosis depends on the stage at diagnosis: the 5-year survival rate is 65% for localized NSCLC but only 9% for distant-stage disease. Radiologists face challenges distinguishing benign from malignant pulmonary nodules on computed tomography scans. This review explores deep learning (DL) methods, including multi-view convolutional neural networks (CNNs) and 3D models for nodule segmentation, emphasizing volumetric assessments for malignancy prediction. CNNs effectively analyze CT data, achieving 94.2% sensitivity with 1.0 false positives per scan in lung nodule detection. DL enhances diagnostic accuracy, reduces radiologist workload, and enables earlier lung cancer detection. Further research is needed to improve model adaptability across diverse clinical settings.

**Key words:** malignant tumor, pathology, morphological detection, radiology and oncology.

## Introduction

Lung cancer is one of the most deadly malignancies that can endanger a person's life or health [1]. Many nations have seen lung cancer incidence and death rise during the last 50 years [2]. The American Cancer Society (ACS) projected 608,570 fatalities and 1,898,160 new cases in 2021 [3]. As a prominent radiological signal, lung nodules are used to diagnose lung cancer early. Diameter determines nodule malignancy [4]. Nodules in the pulmonary interstitium, which consists of the basement membrane, pulmonary capillary endothelium, alveolar epithelium, and perilymphatic and perivascular tissues, are typically small, spherical, and circumscribed [5, 6]. Lung nodules vary in size, shape, and kind [7]. Nodules can vary in size from less than 2 mm to 30 mm, and some are difficult to detect because of their complex circulatory connections in places with numerous vessels [8]. There are certain solid and sub-solid nodules (SSNs) with densities that are marginally greater than those of the parenchyma of the lung [9]. Solid nodules (SNs) are the most common nodules and comprise the core functioning lung tissues, while SSNs

often represent early-stage lung cancers appearing as areas of partial ground-glass opacity. SSNs may be part-solid or pure ground-glass nodules [10]. These nodules do not obscure the broncho-vascular structures, but their opacities are denser than those of the surrounding tissues [7].

Accurate nodule diameter measurements are essential for diagnosis since nodule size is correlated with malignancy. Several studies [5, 11, 12] offer valuable insights [13]. The End-Use Load and Consumer Assessment Program (ELCAP) database [3] reports a 1% malignancy risk for nodules under 5 mm, 24% for 6–10 mm, 33% for 11–20 mm, and 80% for 20+ mm [14]. However, measuring the diameters of extremely small nodules may result in errors. The therapy for cancer of the lung nodules is complicated. Almost 70% of individuals with lung cancer require radiation treatment; however, radiation-induced lung damage may reduce treatment rates and raise morbidity and death. Radiologists rely on computer-aided diagnostic (CAD) technologies to extract more information from nodules and enhance classification accuracy. CAD systems minimize observational errors, false-negative rates, and medical image interpretation and diagnostic second opinions [15, 16]. Numerous studies indicate that CAD systems improve image diagnosis, with lower inter-observer variance [17]. CAD systems can also quantify clinical decisions such as biopsy recommendations [18], facilitate diagnostic checks, minimize thoracotomies and false-positive biopsies [16, 19], and distinguish tumor malignancies [20, 21]. Clinical success has led to the introduction of CAD models for lung cancer diagnosis. Early diagnosis of lung nodules may improve survival using such devices. Current computed tomography (CT) CAD applications search for spherically distributed lung nodule-like pulmonary densities [15]. Thus, lung nodule screening by CT CAD has become a prominent area of research. Lung nodule detection initially was based on non-machine learning techniques [22–28]. Later, data-driven machine learning-based algorithms [29–34] were developed to delineate the ideal nodule border [35]. Deep learning (DL) inspired algorithms have recently attracted interest because of their precise predictions. Unlike traditional CAD systems, DL-based models can be optimized and applied to vast volumes of data [36]. DL using CNNs has improved pulmonary nodule diagnosis and treatment [37–40]. Three modules of DL are used to recognize, segment, and categorize lung nodules. Detection identifies the nodule, segmentation delineates its voxels, and classification determines whether it is benign or malignant [35].

Lung cancer often remains asymptomatic in its early stages, leading to delayed diagnoses.

When symptoms appear, they frequently include shortness of breath, wheezing, hoarseness, chest pain, coughing up blood, and a persistent cough. Additional signs may involve recurrent respiratory infections, unexplained weight loss, and fatigue. Moreover, these symptoms might differ from person to person and can mimic those of other respiratory disorders [41].

Regarding mortality, lung cancer remains a leading cause of cancer-related deaths globally. For instance, in the United States, an estimated 124,730 lung cancer-related deaths are anticipated for 2025. The mortality rate is significantly higher in older populations, with three-quarters of lung cancer deaths occurring among those aged 65 and older. Increasing survival rates require early detection through screening programs, since lung cancer can often be identified at an advanced stage when there are few available treatment choices [41].

Previous studies have explored the detection approaches for pulmonary nodules [35, 36, 42–48] with various goals. The primary aim of this article is to provide a comprehensive review of deep learning (DL) methodologies employed for pulmonary nodule identification and classification in CT images. This study aims to explore the effectiveness of various DL models, including multi-view convolutional neural networks (CNNs) and 3D architectures, in improving diagnostic accuracy and efficiency in lung cancer screening. Furthermore, it aims to identify current challenges, such as data variability and the need for external validation, and suggest directions for future research to facilitate the integration of these advanced technologies into routine clinical practice. This study introduces a novel deep learning-based system using two 3D models for automated pulmonary nodule detection, aiming to enhance diagnostic accuracy and reduce false positives.

## Nodule detection

Identifying microscopic pulmonary nodules is challenging yet important for lung cancer diagnosis. Chest volumetric CT images exceed 9 million voxels. Five-mm lung nodules occupy 130 voxels, corresponding to about  $1.4 \times 10^{-5}$  of the lung volume [49]. Radiologists may be able to detect these nodules based on their shape, size, density, location, and closeness to adjacent structures. Early CT screening missed 8.9% of malignancies in the NLST CT screening arm [50]. The pathological analysis of biopsy samples is still the most reliable method for identifying and defining pulmonary nodules, even though imaging approaches are significant for their detection. Although having two observers simultaneously read a scan improves diagnostic sensitivity, performing it repeatedly

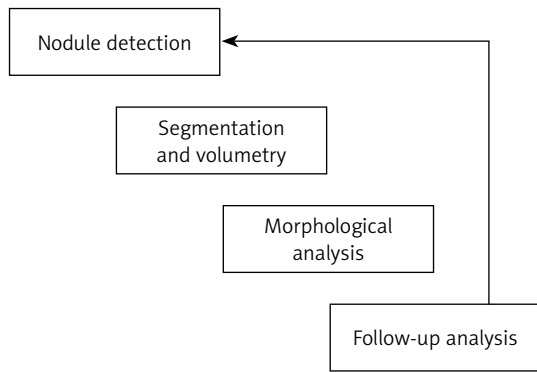


**Figure 1.** Steps in the lung nodule treatment route, where AI might have a role

is time-consuming and impracticable [51]. This emphasizes the significance of machine-learning technology to assist radiologists detect nodules, one of the most studied CAD applications that reduce the time needed to interpret scans [52]. Several studies have demonstrated that deep learning may improve nodule detection sensitivity. Figure 1 shows the steps in the lung nodule treatment route using AI.

This CAD application has been extensively investigated and has been demonstrated to minimize scan interpretation time [52]. Various studies have reported that deep learning can enhance the sensitivity of nodule identification [53].

### Nodule segmentation

Malignancy is strongly predicted by nodule size; in the NELSON trial, those with nodules < 100 mm<sup>3</sup> had the same baseline cancer risk (0.5%) as those without nodules [54]. Traditional nodule size assessment involves manual 2D caliper measurement of the largest transverse diameter. Current screening studies and national and worldwide guidelines on nodule treatment have recommended evaluating volume rather than diameter because it is less susceptible to intra- and interobserver variability [55], better incorporates the three-dimensional (3D) character of a lung nodule [56], is more susceptible to size change, and detects malignancy sooner than 2D diameter measures [57]. Nodule segmentation is essential for volumetric measurements. Numerous CAD methods for nodule segmentation have been developed since the 1980s [44]. Detecting microscopic pulmonary nodules is challenging yet significant for lung cancer diagnosis. Chest volumetric CT images exceed 9 million voxels. Five-mm lung nodules occupy 130 voxels, corresponding to about  $1.4 \times 10^{-5}$  of the lung volume. These nodules may be detectable by radiologists depending on their shape, size, density, location, and proximity to other structures. 16e18 Early CT screening missed

8.9% of malignancies in the NLST CT screening arm [58].

Subsolid nodules are more challenging to segment than solid lesions because there is less attenuation difference between the tumor and the surrounding parenchyma. It is also more challenging to distinguish the solid component of these very large nodules from nearby vessels. However, current research indicates that these problems can be addressed [59]. Multiple manual, semi-automatic, and automated volumetric analysis software programs have been reported in recent years. Although these software tools may produce slightly different size measurements, they provide reliable repeat measurements. The variance is larger in irregular and juxta-pleural nodules [60]. The British Thoracic Society's pulmonary nodule management guidelines suggest reducing variability in nodule volumetry [61].

Research has demonstrated that deep learning can improve nodule segmentation. A single click can volumetrically segment 7,927 NLST nodules using a deep learning model. These parameters were used to evaluate the Brock University Cancer Prediction Model's malignancy prediction accuracy. The AUC for volumetric analysis was 88.17, compared to 85.96 for NLST radiologists' 2D measurements, demonstrating a 2.21% enhancement in predictive value. As CNN algorithms implicitly segment nodules, deep learning may eliminate nodule segmentation [38, 62].

### The issue of detecting lung nodules in daily clinical practice

Lung cancer is the leading cause of cancer death worldwide [63]. Symptoms typically appear after cancer has spread, and therefore late diagnosis is usual [64]. To detect malignancies early, the US, China, and Korea have implemented nationwide lung tumor screening programs. High-risk individuals (older smokers) are invited for a low-dose CT lung scan in a screening program [65]. Lung cancer may manifest as a "nodule" or spot. Trials show that low-dose CT screening reduces lung carcinoma mortality [66, 67], but Europe and other nations have been sluggish in embracing it. Therefore, early-stage lung cancer is often identified incidentally through nodules observed in CT scans carried out for unrelated medical reasons [68, 69]. It can be challenging to detect lung nodules. CT scans are highly heterogeneous and not optimized to identify lung cancer due to the growing diversity of scanning methods and patients [49]. Nodule detection and treatment will become more crucial because radiologists' workload has increased significantly over the past 15 years, primarily due to the demand for CT imaging [70].

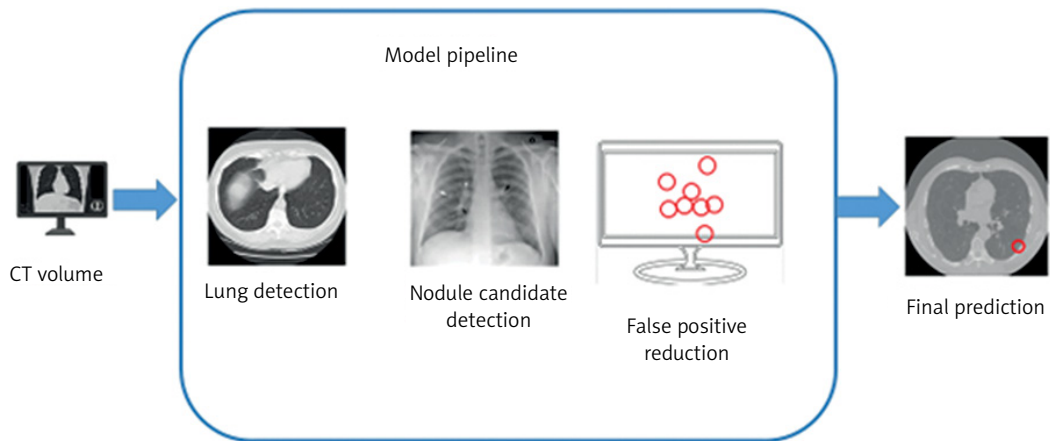


Figure 2. Overview of the planned lung nodule detecting system

### Artificial intelligence for radiological support

AI software may help radiologists find lung lesions in CT images. The use of AI software as an auxiliary reader enhances radiologists' reading time, management recommendation uniformity, and detection sensitivity [71–74]. A few studies have explored AI solutions in non-screening environments. The generalization performance of the AI software was tested using a multi-center study approach to expand this research area and address three common issues. Second, we used five qualified thoracic radiologists rather than one or two to establish the reference standard, because nodule detection varies greatly. Third, and perhaps most importantly, we examined whether an AI system could identify the important nodules using reliable nodule-level malignancy labels. Research on AI has either looked at all nodules (regardless of malignancy) or scan-level cancer detection. Therefore, our effort aims to connect AI investigations for nodule identification and lung malignancy.

### Connecting the gap between nodule detection and lung cancer AI studies

The DL-based technique was retrospectively tested for identifying actionable benign nodules (requiring follow-up), minor lung cancers, and metastases in CT images from two Dutch hospitals' typical clinical contexts. Moreover, the nodule detection method locates a specific lung region slice by slice using a CT scan. Five-slice overlapping CT volumes yield nodule candidates. Finally, nine slices from a 3D area around each nodule candidate are inspected for nodules. Nodules from lung arteries and other structures can be promptly identified in CT scans using the 2.5D identification method (Figure 2).

### DL strategies for detecting lung cancer

Automation has the potential to assist in diagnosing various diseases through CAD [75]. This method employs software to identify, predict, and classify symptoms, assisting in identifying the presence and severity of a disease. This study reviews CAD approaches for lung CT nodule detection. CT scans can identify nodules of lung cancer, especially large ones in the advanced stages [76]. The nodules need to be identified early because they are often very small before a lung tumor the size of a golf ball grows. Figure 3 shows that manually distinguishing and segmenting nodules is challenging.

CNNs are highly effective for image classification. Their architecture is inspired by the human visual system. CNN filters assess a small portion of the image by simulating neurons with receptive zones. Deeper layers of these neurons may learn and detect more complicated hierarchical patterns due to their larger receptive fields. CNNs can be thought of as a collection of sliding windows with small neural networks spread around the image [77].

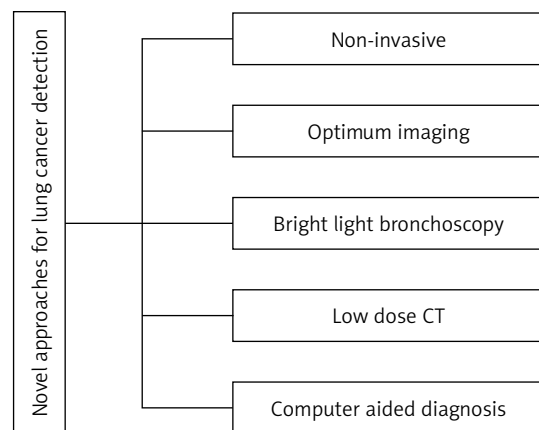


Figure 3. Methods for lung tumor detection

CNNs can learn patterns regardless of location due to their location invariance. The filter can learn image designs using sliding windows. Since CNNs are hierarchical, they can automatically identify more abstract patterns [78]. Boundaries and structures may be occupied by the initial layers, followed by forms in the intermediate layers and overall object shapes in the higher layers. CNNs are capable of analyzing 3D images rather than slices from CT scans. A sliding cube, instead of a movable pane, can be employed to develop 3D CNNs for feature extraction at each stage [79].

### Computer-assisted lung cancer detection using CT images

CT-based lung tumor identification and detection employing DL algorithms has been the subject of numerous studies. Healthy and unhealthy CT scans have different image attenuation patterns. To separate the lungs from the nearby tissues, numerical, grey-level thresholding, and shape-based methods have been employed [80]. Brown and coworkers introduced an automatic, knowledge-based chest segmentation approach [81]. This approach requires organ volume, relative location, shape, and X-ray attenuation. To extract useful CT image data, Brown *et al.* developed a knowledge-based automatic segmentation method [82]. They automatically created indirect quantitative values of single lung activities that routine pulmonary function tests cannot. Hu *et al.* created a completely automated pulmonary segmentation approach from 3D lung X-ray images [83]. The technique was tested employing 3D CT information sets from 8 healthy individuals. Computer and human analysis showed a 0.8-pixel root mean square difference. Lung segmentation was fully automated using a pixel-value threshold based on slices, together with two sets of categorization criteria that incorporate size, circularity, and position data [84]. They achieved 94.0% segmentation precision with 2969 thick slice images and 97.6% with 1161 thin slice images based on 101 CT cases [85]. The lung volume was segmented and visualized using anisotropic filtering and wavelet transform-based interpolation. The robustness and application of the approach were demonstrated using single-detector CT scans, which showed improvements in volume overlap and volume difference percentages.

Swierczynski *et al.* devised a level-set-based segmentation approach that combined traditional segmentation with active dense displaced field prediction [86]. The developed approach outperformed methods that performed registration and segmentation independently. A substitutional level set technique for CT scan lung nodule segmentation was developed using a global lung nod-

ule form model [87]. Nodule kind or position did not affect the proposed technique. Moreover, to improve lung nodule detection, a parameter-free segmentation method was developed that focused on juxtapleural lesions [88]. LIDC's 403 juxtapleural nodules indicated a 92.6% re-inclusion rate. Zhang *et al.* [89] developed an automated lung segmentation approach and a global optimum hybrid geometric active contour model. Incorporating global region and edge information increased algorithm performance in places with narrow bands or weak boundaries. Furthermore, in another study [90], a sphere was placed within the segmented lung target and deformed in response to forces applied to the lung boundaries. The system was tested on 40 CT images, achieving an average F-measure of 99.22%.

Researchers have been examining CNNs' durability in computer vision for 10 years. Multiple CNN-based methods have been reported for medical and natural image processing. Several methods have been proposed using AI and CT images for the detection of lung cancer [91]. Lung nodule classification was carried out using a three-dimensional CNN with three modules. This technique outperformed manual evaluation with 84.4% sensitivity. Nasser and Naser [92] used an ANN to diagnose lung cancer with 96.67% accuracy. Cifci [93] reported that DL, combined with Instantaneously Trained Neural Networks (DITNN) and Increased Profuse Clustering (IPCT), improved lung image quality and lung cancer detection, achieving an accuracy of 98.42%. Moreover, in another study [94], a double convolutional deep neural network (CDNN) and a regular CDNN were employed to identify lung nodules, achieving an accuracy of 0.909 and 0.872.

Wang *et al.* [95] developed a CAD system with low false negative and positive rates as well as high nodule detection precision. In another approach [96], the deep model achieved 95.41% sensitivity in lung image detection using inception-v3 transfer learning instead of randomized initialization. Finally, a multi-group patch-based learning system was reported, revealing an 80.06% sensitivity with 4.7 false positives per scan or a 94% sensitivity with 15.1 false positives per scan. Furthermore, a dense convolutional binary-tree network (DenseBTNet) was developed which showed high parameter effectiveness and extracted features at several scales [97]. Li *et al.* found that early detection reduces the death rate from lung cancer [98]. They developed a DL-CAD system that could recognize and classify lung nodules under 3 mm and estimate their malignancy risk. The system demonstrated an accuracy of 86.2% in sensitivity testing carried out on the LIDC-IDRI and NLST datasets.

Similarly, a deep 3D residual CNN was employed to reduce false positives for automated lung nodule diagnosis in CT images [99]. A spatial pooling and cropping (SPC) layer gathered multi-level contextual information, and their 27-layer network achieved 98.3% sensitivity using the LUNA-16 dataset. Teramoto *et al.* [100] developed a deep convolutional neural network (DCNN) comprising convolutional, completely linked, and pooling layers to automatically classify lung cancer. DCNN training employed 76 cancer cases and achieved 71% classification accuracy. In a study, a 3D convolutional neural network was employed for volumetric CT-based computer-aided lung nodule identification [101]. They used the LUNA16 dataset to test their model, which had 3D convolutional, max-pooling, completely linked, and softmax layers. Their findings suggested that 3D CNNs significantly improved detection accuracy, achieving a sensitivity of 94.4%.

Similarly, DL algorithms were employed to predict lung cancer survival, determine EGFR mutation status, and classify subtypes based on CT scans [102, 103]. Several studies have explored the use of DL algorithms for pulmonary nodule segmentation and categorization in CT imaging [35]. A 3D deep-learning model and low-dose chest CT images were employed to develop an end-to-end lung tumor detection system [104]. Shao *et al.* [105] employed DL algorithms to screen mobile low-dose CT images for lung tumors in resource-constrained areas. Moreover, a model [106] was designed that identified the EGFR mutations and expression of PD-L1 status in non-small-cell lung tumors using CT images. A study [107] provided an in-depth analysis of different DL approaches for identifying and diagnosing lung nodules in CT scans.

Deep neural networks were employed to segment lung CT images [11] in addition to categorization. Lakshmanaprabu *et al.* [108] determined that the DL model achieved the highest classification accuracy of 96.3% for lung tumors using CT data. The application of DL models in chest radiography and lung tumor identification using CT images was investigated by Lee *et al.* [109], who observed that these models may increase clinical efficacy and accuracy. To identify lung cancer, Bhatia *et al.* [110] proposed a DL technique with 93.55% sensitivity and 91.5% specificity. Moreover, another model [111] was designed using DL on CT scans to detect expression of PD-L1 in non-small cell lung tumors and predict immune checkpoint suppressor responses for a smaller nodule. Hu *et al.* [112] proposed a DL system for lung cancer stage extraction from CT data with an F1 score of 0.848. A machine learning strategy that can detect preinvasive, benign, and invasive lung nodules on 1-mm-thick CT scans was proposed

[74, 113] to demonstrate the efficacy of a DL-enhanced CAD system in recognizing them. Deep learning was also used to predict lung cancer with an accuracy of 87.63% [114].

Rajasekar *et al.* [115] developed six DL models (CNN GD, CNN, Inception V3, VGG-16, Resnet-50, and VGG-19) that efficiently identified lung tumors by employing CT scans and histopathology images. CNN-GD outperformed other models in precision, F-score, sensitivity, accuracy, and specificity, achieving 97.86%, 96.39%, 96.79%, and 97.40%, respectively. Wankhade *et al.* [116] presented a 3D-CNN and recurrent neural network (RNN) approach that achieved 95% accuracy in classifying malignant lung nodules. Efficiency can be improved using big-data analytics and cascade classifiers. Abunajm *et al.* [117] proposed a CNN-based model for primary lung cancer prediction and recognition using CT scan imaging, distinguishing malignant, benign, and normal cases. Initial lung cancer detection improves survival and timing of therapy. The model reduced false positives and achieved an accuracy of 99.45%.

In a study [118], radiomics and deep learning were employed for lung cancer identification and treatment. Experts explain that radiomics enables the quantification of medical images, enhancing cancer diagnosis and prognosis. Deep learning systems can be used for data analysis. Deep learning was used to forecast the risk of cardiovascular disorders from low-dose CT scans used to test for lung tumors [119]. The researchers used a massive cardiovascular risk dataset to train a DL system to predict heart disease risk from lung CT images. Moreover, in a study [120], dense clustering and DL were combined to immediately train neural networks to improve lung tumor detection from CT images. They demonstrated the efficiency of their lung nodule detection approach by comparing it with existing lung cancer detection methods. A newly developed DCNN was assessed on a large dataset of CT scans to detect and classify lung nodules in 3D CT images [121]. Zhao *et al.* [122] proposed a weighted discriminatory extreme learning machine for electronic nasal system lung tumor detection. They were able to differentiate between the two groups by using an electronic nasal device to examine breath samples from lung tumor patients and healthy controls. Chen *et al.* [123] developed a multimodality attention-guided 3D detection system for non-small cell lung cancer using 18 F-FDG PET/CT images. The accuracy of PET/CT lung cancer detection was improved by the researchers using deep learning algorithms, which could help in early diagnosis and treatment. Table I lists the uses, advantages, and drawbacks of lung imaging technologies, while Table II lists the models studied between 2018 and 2022.

### Developing techniques for detecting lung cancer

Lung cancer is a highly fatal form of cancer. Identifying cases is challenging because they typically

manifest in the terminal stage. However, mortality can be reduced by early disease detection and treatment. CT imaging is a reliable diagnostic method since it can detect all predicted and unexpected lung tumor nodules [124]. However, medical

**Table I.** Uses, advantages, and drawbacks of lung imaging technologies

Technology	Uses	Advantages	Drawbacks
CT Imaging	Primary detection of lung tumors; segmentation of lung nodules.	High-resolution imaging; clear separation of lung vs. non-lung areas due to attenuation differences.	Susceptible to heterogeneity, poor contrast variations, noise, and difficulty distinguishing benign from malignant nodules.
MRI Imaging	Delineation of organ/lesion boundaries; morphological assessment.	Improved soft tissue contrast.	Lower spatial resolution for lung structures; higher sensitivity to motion artifacts; less commonly used for lung nodule detection.
EBUS (Endobronchial Ultrasound)	Visualization of internal lung structures; assisting in tumor characterization.	Minimally invasive; provides real-time imaging.	Limited research on CNN interpretation; challenges in differentiating benign from malignant lesions.
Traditional CADx Systems	Automated analysis using hand-crafted features.	Established methodology; less computationally intensive.	Lower accuracy compared to DL-based methods; reliance on manually engineered features that are less robust and adaptable.

**Table II.** Studied models for lung image segmentation and nodule detection (2018–2022)

Model/study	Architecture/method	Key features/performance
Basic CNN Model for Lung Segmentation	Single convolution layer (6 kernels), max pooling, 2 fully connected layers; clustering-based training dataset.	Utilizes k-means clustering for dataset creation; evaluated via eightfold cross-validation.
Automated Lung Segmentation via Image Decomposition & Filtering	Combination of image decomposition-based filtering, wavelet transformation, and morphological methods with contour correction.	Denoises CT images while preserving lung outlines.
Residual U-Net for Lung CT Segmentation	Residual U-Net incorporating residual units.	Designed to reduce false positives and extract robust segmentation features.
U-Net vs. E-Net Comparison for Pulmonary Fibrosis Segmentation	Comparative study between U-Net and E-Net architectures.	Achieves fast and effective segmentation of pulmonary fibrosis parenchyma.
U-Net-Based Lung Segmentation with Dual Paths	U-Net variant featuring an expanding path for high-level and contracting path for low-level information.	High segmentation accuracy with a Dice coefficient of 0.9502.
Mask R-CNN-Based Lung Segmentation	Mask R-CNN integrated with supervised and unsupervised machine learning.	Rapid segmentation (11.2 s) with high precision (97.68%).
Multi-View Convolutional Network for Nodule Recognition	Integration of several 2D ConvNet streams with a reliable classification algorithm.	Targets solid, subsolid, and large nodules; 85.4% detection sensitivity with 4 false positives per scan.
3D CNN and FCN for Autonomous Nodule Identification	3D CNN combined with a fully convolutional network (FCN).	Rapid generation of volume score maps; autonomous detection of candidate regions.
Deep Learning with Shape-Driven Level Sets	Combination of deep learning and level set methods for segmentation.	Automatic fine segmentation is initialized by seed points from coarse segmentation.

practitioners and radiologists may misinterpret CT scan intensity and anatomical structure, making malignant cell identification difficult [125]. Therefore, computer-aided diagnostic methods are being employed by radiologists and physicians to diagnose cancer [126]. Numerous technologies have been established, and research into lung cancer detection is still ongoing. Certain systems need to be improved to achieve 100% detection accuracy.

Lung cancer may be cured with the correct medications, early detection, and a precise etiology. Early lung tumor detection is therefore essential, especially when screening high-risk populations such as oil field workers, smokers, individuals exposed to fumes, and others, for whom new biomarkers are required. The precision of the diagnosis also affects the best course of treatment for lung cancer. Therefore, finding sensitive and precise biomarkers is essential for primary diagnosis. Low-dose CT is used in recent lung cancer screening methods. Compared to cases without screening, the NELSON trial [127] reported that this screening method provides 85% sensitivity and 99% specificity. A recent study [128] demonstrated a false-positive rate of less than 81%, necessitating further imaging or testing due to the high incidence.

To explain the lung cancer stage and screening schedule, a brief overview is given here. SCLC and NSCLC are the primary lung cancer subtypes. SCLCs are central tumors that form airway submucosal perihilar masses. Histological studies show that basal bronchial epithelial neuroendocrine cells cause this malignancy. Most cells in this scenario are spindle-shaped, rounded, or small with minimal granular chromatin, cytoplasm, and necrosis [129]. Unlike pure and mixed NSCLC, which may include liver, brain, and bone metastases [130], SCLC has limited or extensive phases [131].

This malignancy [132] may be characterized by metastases to the brain, liver, and bones, with its stages classified as either confined or extensive [133]. Limited SCLC includes the ipsilateral mediastinum, mediastinal, or supraclavicular lymph nodes at a single radiation site. It is a supraclavicular lymph node if it is located on the same side as the cancerous chest. However, broad SCLC can extend to the second lung lobe, bone marrow, and lymph nodes. Chest radiography produces more detailed images than a chest CT scan, but it is less sensitive. With these characteristics, a computer-aided diagnostic (CAD) model for chest radiographs would improve detection sensitivity while preserving low false-positive (FP) rates [134].

Cytological analysis of sputum, especially many samples, may help diagnose lung cancer and find a core tumor in the larger bronchi. Sputum samples seldom include very small adenocarcinomas

under 2 cm that originate from airway branches such as the bronchi, bronchioles, and alveoli [135]. As cigarette exposure has influenced the incidence of squamous cell carcinomas and adenocarcinomas, this information has become more and more crucial. Several screening investigations found that sputum cytology had a 20–30% sensitivity for primary lung tumors. Early studies found that the quantity and form of cells in deeper airways can alter pre-malignant detection [136]. It was reported [137] that regular sputum cytology is neither sensitive nor precise for lung cancer screening. White light bronchoscopy is the most common histological lung cancer diagnosis procedure. Bronchoscopy can detect pre-malignant lesions. Tissue biopsy remains the standard method for detecting cancer in general hospitals. The size of lung tissue biopsy specimens is crucial for the histopathological detection of lung cancer subtypes. The first biopsy needs to confirm the diagnosis to avoid recurrent operations that may cause difficulties and delay therapy. Fiber-optic bronchoscopy, image-guided trans-thoracic needle aspiration, endobronchial ultrasound, pleural fluid examination (thoracentesis), mediastinoscopy, thoracoscopy, and operations are employed to diagnose lung tumors. These methods are expensive, error-prone, and need numerous samples [138].

Spiral CT images enhance the performance of peripheral small tumor diagnosis. However, these images show significantly reduced sensitivity for central tumor identification (primarily squamous cell carcinoma) than peripheral tumors [139]. In the National Lung Screening Trial (NLST) using low-dose CT (LDCT), 96% of positive screenings were false positives, with over 40% of participants experiencing at least one positive result [66]. The high frequency of false positive screening results in expensive and intrusive therapies for smokers without malignancies. For diagnosis, screening for lung cancer with low-cost, non-invasive methods is essential.

CNN, a kind of DL, has advanced radiology [140, 141]. In chest radiography, DL-based models have also demonstrated success in detecting masses and nodules, with mean false positives per image (mFPIs) of 0.02–0.34 and sensitivities of 0.51–0.84. Moreover, radiologists were able to identify nodules more accurately with CAD models than with screening procedures without them. It can be difficult for radiologists to identify and differentiate between benign and malignant nodules [142, 143]. Radiologists also need to monitor nodule form and marginal features as typical anatomical structures mimic healthy nodules. Even the most skilled radiologists may make diagnostic mistakes due to circumstances rather than their

own shortcomings [144, 145]. The main DL methods for lesion identification are segmentation and detection. The detection approach labels an area, unlike the segmentation method, which labels pixels. Segmentation provides more exact pixel labels than detection. Pixel-level lesion size categorization enhances clinical diagnosis. Lesion size and form variations are easier to monitor using pixel-level classification because the shape may affect detection. As part of the evaluation of management effectiveness, it also displays lesion size and long and short diameters [146].

### Investigation gaps and limitations

Better survival rates depend on the primary detection of lung tumors; however, this is difficult because of factors such as heterogeneity, low contrast fluctuations, and visual similarities between benign and malignant nodules in CT images [147]. Identifying lung nodules with medical imaging is challenging owing to the complex architecture and time-consuming acquisition of labeled samples [148]. Deep learning algorithms are frequently compared to traditional CAD systems that employ manually created features, even though they can automatically identify features in lung nodule CT scans [149]. There is limited research on employing CNNs to analyze EBUS images, which makes it challenging to distinguish benign from potentially malignant tumors [150]. While some studies have employed CT scans to predict mortality risks in NSCLC patients, they have not identified primary-stage lung or lobe-related malignancies [151]. The mechanism by which CNNs predict nodule malignancy and the influence of area or contextual information on their output remains unclear [152]. Computer-assisted lung disease detection is crucial owing to noise signals affecting cancer image quality during acquisition [153]. Training DCNNs is challenging because of the various kinds of lung nodules and limited availability of positive samples in many datasets [154].

### Segmentation process

Image segmentation shows organ or structural outlines. DL techniques improve semantic segmentation, which makes them useful for medical diagnosis. This method evaluates the sizes and shapes of organs or lesions using MRI or CT scans [155, 156]. Many researchers have proposed automated segmentation methods. However, pre-processing typically involves edge detection and the application of mathematical filters. Further, deep machine learning extracted complex traits. Creating and extracting hand-crafted features was the biggest challenge for such a system, limiting deployment. Medical researchers segmented images

using 2D, 2.5D, and 3D CNN [157, 158]. A CT scan can easily separate the lung and non-lung areas in a typical lung due to their different image attenuation. Early lung segmentation approaches encompassed numerical methods, gray-level thresholding, and shape-based approaches to distinguish lung regions from non-lung areas.

Various CNN-based methods have been established for both medical and natural image processing. Early research focused on lung nodule segmentation [156]. In a study [159], a basic CNN model for lung segmentation was developed employing a clustering algorithm-based training dataset. The k-means clustering technique divided CT slices into two groups using the image patch's mean and minimum intensity. Cross-shaped confirmation, volume intersection, linked component analysis, and patch expansion were used to construct the dataset. The CNN design comprised a single layer of convolution with 6 kernels, one maximally pooled layer, and two fully connected layers. An eightfold cross-validation method was employed to evaluate CNN models trained on the produced datasets. The researchers designed automated lung segmentation techniques to denoise lung CT images without affecting lung outlines using an image decomposition-based filtering technique [160]. The lungs were segmented using wavelet transformation and morphological methods. Finally, contour correction was used to smooth the lung outlines during segmentation refinement.

Khanna *et al.* [161] developed a false-positive-reducing Residual U-Net for lung CT segmentation. The more complex network with residual units in the suggested model makes it easier to extract lung segmentation information. Performance comparisons of U-Net and E-Net were also performed [162]. These models partition pulmonary fibrosis parenchyma quickly and effectively.

Furthermore, a U-Net-based lung segmentation approach was developed that had an expanding route for high-level information and a contracting route for low-level information [163]. The model achieved a Dice coefficient of 0.9502 in the experiments. Mask R-CNN and supervised and unsupervised machine learning were used to produce another automated lung segmentation method [164]. The benchmarked methods were slower and less precise than our approach, which achieved a segmentation precision of 97.68% and was completed in 11.2 s.

Setio *et al.* presented a multi-view convolution network to recognize lung nodules using discriminative features of training data [165]. The three-nodule potential detectors target solid, subsolid, and large nodules. The proposed method integrates several 2-D ConvNet streams with a reliable clas-

sification algorithm. The LIDC-IDRI dataset shows four false positives per scan and 85.4% detection sensitivity. Similarly, a 3D CNN was trained using LIDC dataset volumes of interest to autonomously identify lung nodules [166]. Furthermore, a 3D CNN was employed to quickly produce the volume score map in a single run by generating a 3D fully convolutional network (FCN). Candidate regions of interest were quickly generated by the discriminating CNN using the FCN-based architecture.

In another study [167], DL and shape-driven level sets were employed to produce another automatic lung nodule segmentation system. The invention of shape-driven level sets was the first step toward fine segmentation. Similarly, the model was automatically initialized by the level sets using seed points from the deep network's coarse segmentation.

### Conclusion and recommendations

This study highlights the significant progress made in pulmonary nodule diagnosis and segmentation through deep learning (DL) techniques. The study addresses issues including heterogeneity, low contrast variations, and the visual similarities between benign and malignant formations in CT imaging by using CNNs and transfers learning techniques to improve the accuracy of lung nodule identification and delineation. The integration of DL approaches has shown superiority over traditional computer-aided diagnostic (CAD) systems that rely on hand-crafted features, offering a more robust and automated solution for early lung cancer detection.

For future research, a deeper exploration of DL model interpretability is crucial to clarify the specific features and contextual information these networks use to distinguish between benign and malignant nodules. Furthermore, expanding the diversity and size of annotated datasets will enhance the generalizability and performance of DL models. Collaborative efforts between multidisciplinary teams, including radiologists, data scientists, and clinicians, are essential to translate these technological advancements into clinical practice, ultimately improving patient outcomes through early and accurate lung cancer diagnosis.

### Funding

No external funding.

### Ethical approval

Not applicable.

### Conflict of interest

The authors declare no conflict of interest.

### References

1. Gałązka JK, Czeczulewski M, Kucharczyk T, et al. Obesity and lung cancer – is programmed death ligand-1 (PD-1L) expression a connection? *Arch Med Sci* 2024; 20: 313-6.
2. Thandra KC, Barsouk A, Saginala K, et al. Epidemiology of lung cancer. *Contemp Oncol (Pozn)* 2021; 25: 45-52.
3. Siegel RL, Miller KD, Fuchs HE, et al. *Cancer Statistics, 2021*. *CA Cancer J Clin* 2021; 71: 7-33.
4. Gould MK, Donington J, Lynch WR, et al. Evaluation of individuals with pulmonary nodules: when is it lung cancer? Diagnosis and management of lung cancer, 3rd ed: American College of Chest Physicians evidence-based clinical practice guidelines. *Chest* 2013; 143 (5 Suppl): e93S-120S.
5. Bankier AA, MacMahon H, Goo JM, et al. Recommendations for measuring pulmonary nodules at CT: a statement from the Fleischner society. *Radiology* 2017; 285: 584-600.
6. Hansell DM, Bankier AA, MacMahon H, et al. Fleischner Society: glossary of terms for thoracic imaging. *Radiology* 2008; 246: 697-722.
7. Lu MS, Chen MF, Yang YH, et al. Appraisal of lung cancer survival in patients with end-stage renal disease. *Arch Med Sci* 2023; 19: 86-93.
8. Choi WJ, Choi TS. Automated pulmonary nodule detection based on three-dimensional shape-based feature descriptor. *Comput Methods Programs Biomed* 2014; 113: 37-54.
9. Peloschek P, Sailer J, Weber M, et al. Pulmonary nodules: sensitivity of maximum intensity projection versus that of volume rendering of 3D multidetector CT data. *Radiology* 2007; 243: 561-9.
10. Kim H, Park CM, Koh JM, et al. Pulmonary subsolid nodules: what radiologists need to know about the imaging features and management strategy. *Diagn Interv Radiol* 2014; 20: 47-57.
11. Revel MP, Bissery A, Bienvenu M, et al. Are two-dimensional CT measurements of small noncalcified pulmonary nodules reliable? *Radiology* 2004; 231: 453-8.
12. Han D, Heuvelmans MA, Oudkerk M. Volume versus diameter assessment of small pulmonary nodules in CT lung cancer screening. *Transl Lung Cancer Res* 2017; 6: 52.
13. Brzozowska M, Wierzbę W, Szafraniec-Buryto S, et al. Overall survival of patients with EGFR mutation-positive non-small-cell lung cancer treated with erlotinib, gefitinib or afatinib under drug programmes in Poland – real-world data. *Arch Med Sci* 2021; 17: 1618-27.
14. Henschke CI. Early lung cancer action project: overall design and findings from baseline screening. *Lancet* 1999; 354: 99-105.
15. Castellino RA. Computer aided detection (CAD): an overview. *Cancer Imaging* 2005; 5: 17.
16. McCarville MB, Lederman HM, Santana VM, et al. Distinguishing benign from malignant pulmonary nodules with helical chest CT in children with malignant solid tumors. *Radiology* 2006; 239: 514-20.
17. Singh S, Maxwell J, Baker JA, et al. Computer-aided classification of breast masses: performance and interobserver variability of expert radiologists versus residents. *Radiology* 2011; 258: 73-80.
18. Giger ML, Karssemeijer N, Schnabel JA. Breast image analysis for risk assessment, detection, diagnosis, and treatment of cancer. *Annu Rev Biomed Eng* 2013; 15: 327-57.
19. Joo S, Yang Y, Moon WK, Kim HC. Computer-aided diagnosis of solid breast nodules: use of an artificial neural

- network based on multi pleonographic features. *IEEE Transact Med Imaging* 2004; 23: 1292-300.
20. Way TW, Sahiner B, Chan HP, et al. Computer-aided diagnosis of pulmonary nodules on CT scans: improvement of classification performance with nodule surface features. *Med Phys* 2009; 36: 3086-98.
  21. Way TW, Hadjiiski LM, Sahiner B, et al. Computer-aided diagnosis of pulmonary nodules on CT scans: segmentation and classification using 3D active contours. *Med Phys* 2006; 33: 2323-37.
  22. Giger ML, Ahn N, Doi K, et al. Computerized detection of pulmonary nodules in digital chest images: use of morphological filters in reducing false-positive detections. *Med Phys* 1990; 17: 861-5.
  23. Ying W, Cunxi C, Tong J, et al. Segmentation of regions of interest in lung CT images based on 2-D OTSU optimized by genetic algorithm in 2009 Chinese Control and Decision Conference. *IEEE* 2009: 5185-9.
  24. Helen R, Kamaraj N, Selvi K, et al. Segmentation of pulmonary parenchyma in CT lung images based on 2D Otsu optimized by PSO. in 2011 international conference on emerging trends in electrical and computer technology. *IEEE* 2011; 536-54.
  25. Liu Y, Wang Z, Guo M, et al. Hidden conditional random field for lung nodule detection. in 2014 IEEE International Conference on Image Processing (ICIP). *IEEE* 2014; 3518-21.
  26. John J, Mini M. Multilevel thresholding based segmentation and feature extraction for pulmonary nodule detection. *Procedia Technolog* 2016; 24: 957-63.
  27. Teramoto A, Fujita H, Yamamuro O, et al. Automated detection of pulmonary nodules in PET/CT images: ensemble false-positive reduction using a convolutional neural network technique. *Med Phys* 2016; 43: 2821-7.
  28. Mastouri R, Neji H, Hantous-Zannad S, et al. A morphological operation-based approach for Sub-pleural lung nodule detection from CT images. in 2018 IEEE 4th Middle East Conference on Biomedical Engineering (MECBME). *IEEE* 2018; 84-89.
  29. Santos AM, de Carvalho Filho AO, Silva AC, et al. Automatic detection of small lung nodules in 3D CT data using Gaussian mixture models, Tsallis entropy and SVM. *Eng Appl Artif Intell* 2014; 36: 27-39.
  30. Madero Orozco H, Vergara Villegas OO, Cruz Sanchez VG, et al. Automated system for lung nodules classification based on wavelet feature descriptor and support vector machine. *Biomed Eng Online* 2015; 14: 9.
  31. Lu L, Tan Y, Schwartz LH, et al. Hybrid detection of lung nodules on CT scan images. *Med Phys* 2015; 42: 5042-54.
  32. Farahani FV, Ahmadi A, Zarandi MF. Lung nodule diagnosis from CT images based on ensemble learning. in 2015 IEEE Conference on Computational Intelligence in Bioinformatics and Computational Biology (CIBCB). *IEEE* 2015; 1-7.
  33. Klik MA, Rikxoort EM, Peters JF, et al. Improved classification of pulmonary nodules by automated detection of benign subpleural lymph nodes. in 3rd IEEE International Symposium on Biomedical Imaging: Nano to Macro. *IEEE* 2006: 494-7.
  34. Froz BR, de C. Filhoa AO, Silva AC, et al. Lung nodule classification using artificial crawlers, directional texture and support vector machine. *Expert Syst Appl* 2017; 69: 176-88.
  35. Wu J, Qian T. A survey of pulmonary nodule detection, segmentation and classification in computed tomography with deep learning techniques. *J Med Artif Intell* 2019; 2.
  36. Liu K, Li Q, Ma J, et al. Evaluating a fully automated pulmonary nodule detection approach and its impact on radiologist performance. *Radiol Artif Intell* 2019; 1: e180084.
  37. Shen W, Zhou M, Yang F, et al. Multi-scale convolutional neural networks for lung nodule classification. In: *International conference on information processing in medical imaging* 2015; 588-599. Cham: Springer International Publishing.
  38. Ciompi F, Chung K, Van Riel SJ, et al. Towards automatic pulmonary nodule management in lung cancer screening with deep learning. *Sci Rep* 2017; 7: 46479.
  39. Causey JL, Zhang J, Ma S, et al. Highly accurate model for prediction of lung nodule malignancy with CT scans. *Sci Rep* 2018; 8: 9286.
  40. Hua KL, Hsu CH, Hidayati SC, et al. Computer-aided classification of lung nodules on computed tomography images via deep learning technique. *Onco Targets Ther* 2015; 4: 2015-22.
  41. Hensley CP, Emerson AJ. Non-small cell lung carcinoma: clinical reasoning in the management of a patient referred to physical therapy for costochondritis. *Phys Ther* 2018; 98: 503-9.
  42. Dhara AK, Mukhopadhyay S, Khandelwal N, et al. Computer-aided detection and analysis of pulmonary nodule from CT images: a survey. *IETE Tech Rev* 2012; 29: 265-75.
  43. Sluimer I, Schilham A, Prokopet M, et al. Computer analysis of computed tomography scans of the lung: a survey. *IEEE Trans Med Imaging* 2006; 25: 385-405.
  44. Valente IRS, Cortez PC, Neto EC, et al. Automatic 3D pulmonary nodule detection in CT images: a survey. *Comput Methods Programs Biomed* 2016; 124: 91-107.
  45. Amitava H, Dey D, Sadhu AK. Lung nodule detection from feature engineering to deep learning in thoracic CT images: a comprehensive review. *J Digit Imaging* 2020; 33: 655-77.
  46. Guobin Z, Jiang S, Yang Z, et al. Automatic nodule detection for lung cancer in CT images: a review. *Comput Biol Med* 2018; 103: 287-300.
  47. Yu G, Chi J, Liu J, et al. A survey of computer-aided diagnosis of lung nodules from CT scans using deep learning. *Comput Biol Med* 2021; 137: 104806.
  48. Patrice M, Qi S, Ma H, et al. Detection and classification of pulmonary nodules using convolutional neural networks: a survey. *IEEE Access* 2019; 7: 78075-91.
  49. Rubin GD. Lung nodule and cancer detection in computed tomography screening. *J Thorac Imaging* 2015; 30: 130-8.
  50. Th SE, Horeweg N, de Koning HJ, et al. Computed tomographic characteristics of interval and post-screen carcinomas in lung cancer screening. *Eur Radiol* 2015; 25: 81-8.
  51. Arjun N, Screamon NJ, Holemans JA, et al. The impact of trained radiographers as concurrent readers on performance and reading time of experienced radiologists in the UK Lung Cancer Screening (UKLS) trial. *Eur Radiol* 2018; 28: 226-34.
  52. Matsumoto S, Ohno Y, Aoki T, et al. Computer-aided detection of lung nodules on multidetector CT in concurrent-reader and second-reader modes: a comparative study. *Eur Radiol* 2013; 82: 1332-7.
  53. Yixin Y, Feng X, Chi W, et al. Deep learning aided decision support for pulmonary nodules diagnosing: a review. *J Thorac Dis* 2018; 10: S867.
  54. Nanda H, Scholten ET, de Jong PA, et al. Detection of lung cancer through low-dose CT screening (NELSON):

- a prespecified analysis of screening test performance and interval cancers. *Lancet Oncol* 2014; 15: 1342-50.
55. Goo JM. A computer-aided diagnosis for evaluating lung nodules on chest CT: the current status and perspective. *Korean J Radiol* 2011; 12: 145-55.
  56. Korst RJ, Lee BE, Krinsky GA, et al. The utility of automated volumetric growth analysis in a dedicated pulmonary nodule clinic. *J Thorac Cardiovasc Surg* 2011; 142: 372-7.
  57. Ko JP, Berman EJ, Kaur M, et al. Pulmonary nodules: growth rate assessment in patients by using serial CT and three-dimensional volumetry. *Radiology* 2012; 262: 662-71.
  58. Kuhnigk JM, Dicken V, Bornemann L, et al. Morphological segmentation and partial volume analysis for volumetry of solid pulmonary lesions in thoracic CT scans. *IEEE Trans Med Imaging* 2006; 25: 417-34.
  59. Devaraj A, van Ginneken B, Nair A, et al. Use of volumetry for lung nodule management: theory and practice. *Radiology* 2017; 284: 630-44.
  60. de Hoop B, Gietema H, van Ginneken B, et al. A comparison of six software packages for evaluation of solid lung nodules using semi-automated volumetry: what is the minimum increase in size to detect growth in repeated CT examinations. *Eur Radiol* 2009; 19: 800-8.
  61. Callister MEJ, Baldwin DR, Akram AR, et al. British Thoracic Society guidelines for the investigation and management of pulmonary nodules: accredited by NICE. *Thorax* 2015; 70 (Suppl 2): ii1-54.
  62. Kadir T, Gleeson F. Lung cancer prediction using machine learning and advanced imaging techniques. *Transl Lung Cancer Res* 2018; 7: 304-12.
  63. Sung H, Ferlay J, Siegel RL, et al. Global cancer statistics 2020: GLOBOCAN estimates of incidence and mortality worldwide for 36 cancers in 185 countries. *CA Cancer J Clin* 2021; 71: 209-49.
  64. Birring SS, Peake MD. Symptoms and the early diagnosis of lung cancer. *Thorax* 2005; 60: 268-9.
  65. Cataldo JK. High-risk older smokers' perceptions, attitudes, and beliefs about lung cancer screening. *Cancer Med* 2016; 5: 753-9.
  66. National Lung Screening Trial Research Team. Reduced lung-cancer mortality with low-dose computed tomographic screening. *N Engl J Med* 2011; 365: 395-409.
  67. de Koning HJ, van der Aalst CM, de Jong PA, et al. Reduced lung-cancer mortality with volume CT screening in a randomized trial. *N Engl J Med* 2020; 382: 503-13.
  68. Gould MK, Tang T, Liu IA, et al. Recent trends in the identification of incidental pulmonary nodules. *Am J Respir Crit Care Med* 2015; 192: 1208-14.
  69. Hendrix W, Rutten M, Hendrix N, et al. Trends in the incidence of pulmonary nodules in chest computed tomography: 10-year results from two Dutch hospitals. *Eur Radiol* 2023; 33: 8279-88.
  70. Bruls RJM, Kwee RM. Workload for radiologists during on-call hours: dramatic increase in the past 15 years. *Insights Imaging* 2020; 11: 121.
  71. Murchison JT, Ritchie G, Senyszak D, et al. Validation of a deep learning computer-aided system for CT-based lung nodule detection, classification, and growth rate estimation in a routine clinical population. *PLoS One* 2022; 17: e026679.
  72. Jacobs C, Schreuder A, van Riel SJ, et al. Assisted versus manual interpretation of low-dose CT scans for lung cancer screening: impact on lung-RADS agreement. *Radiol Imaging Cancer* 2021; 3: e200160.
  73. Hempel HL, Engbersen MP, Wakkie J, et al. Higher agreement between readers with deep learning CAD software for reporting pulmonary nodules on CT. *Eur J Radiol Open* 2022; 9: 10043.
  74. Kozuka T, Matsukubo Y, Kadoba T, et al. Efficiency of a computer-aided diagnosis (CAD) system with deep learning in detection of pulmonary nodules on 1-mm-thick images of computed tomography. *Jpn J Radiol* 2020; 38: 1052-61.
  75. Cellina M, Cacioppa LM, Ce M, et al. Artificial intelligence in lung cancer screening: the future is now. *Cancers* 2023; 15: 4344.
  76. Way T, Chan H, Hadjiiski L, et al. Computer-aided diagnosis of lung nodules on CT scans: ROC study of its effect on radiologists' performance. *Acad Radiol* 2010; 17: 323-32.
  77. Vu H, Kim HC, Jung M, et al. fMRI volume classification using a 3D convolutional neural network robust to shifted and scaled neuronal activations. *Neuroimage* 2020; 223: 117328.
  78. Celeghin A, Borriero A, Orsenigo D, et al. Convolutional neural networks for vision neuroscience: significance, developments, and outstanding issues. *Front Comput Neurosci* 2023; 17: 1153572.
  79. Lundervold AS, Lundervold A. An overview of deep learning in medical imaging focusing on MRI. *Z Med Phys* 2019; 29: 102-27.
  80. Thanoon MA, Zulkifley MA, Mohd Zainuri MAA, et al. A review of deep learning techniques for lung cancer screening and diagnosis based on CT images. *Diagnostics* 2023; 13: 2617.
  81. Brown MS, McNitt-Gray MF, Mankovich NJ, et al. Method for segmenting chest CT image data using an anatomical model: preliminary results. *IEEE Trans Med Imaging* 2002; 16: 828-39.
  82. Brown MS, Goldin JG, McNitt-Gray MF, et al. Knowledge-based segmentation of thoracic computed tomography images for assessment of split lung function. *Med Phys* 2000; 27: 592-8.
  83. Hu S, Hoffman EA, Reinhardt JM. Automatic lung segmentation for accurate quantitation of volumetric X-ray CT images. *IEEE Trans Med Imaging* 2001; 20: 490-8.
  84. Leader JK, Zheng B, Rogers RM, et al. Automated lung segmentation in X-ray computed tomography: development and evaluation of a heuristic threshold-based scheme. *Acad Radiol* 2003; 10: 1224-36.
  85. Sun X, Zhang H, Duan H. 3D computerized segmentation of lung volume with computed tomography. *Acad Radiol* 2006; 13: 670-7.
  86. Swierczynski P, Papież BW, Schnabel JA, et al. A level-set approach to joint image segmentation and registration with application to CT lung imaging. *Comput Med Imaging Graph* 2018; 65: 58-68.
  87. Farag AA, Abd El Munim HE, Graham JH, et al. A novel approach for lung nodules segmentation in chest CT using level sets. *IEEE Trans Image Process* 2013; 22: 5202-13.
  88. Shen S, Bui AA, Cong J, et al. An automated lung segmentation approach using bidirectional chain codes to improve nodule detection accuracy. *Comput Biol Med* 2015; 57: 139-49.
  89. Zhang W, Wang X, Zhang P, et al. Global optimal hybrid geometric active contour for automated lung segmentation on CT images. *Comput Biol Med* 2017; 91: 168-80.
  90. Rebouças Filho PP, Cortez PC, da Silva Barros AC, et al. Novel and powerful 3D adaptive crisp active contour

- method applied in the segmentation of CT lung images. *Med Image Anal* 2017; 35: 503-16.
91. Zhang C, Sun X, Dang K, et al. Toward an expert level of lung cancer detection and classification using a deep convolutional neural network. *Oncologist* 2019; 24: 1159-65.
  92. Nasser IM, Abu-Naser SS. Lung cancer detection using an artificial neural network. *Int J Eng Inf Syst* 2019; 3: 17-23.
  93. Cifci MA. SegChaNet: a novel model for lung cancer segmentation in CT scans. *Appl Bionics Biomech* 2022; 2022: 1139587.
  94. Jakimovski G, Davcev D. Using double convolution neural network for lung cancer stage detection. *Appl Sci* 2019; 9: 427.
  95. Wang J, Wang J, Wen Y, et al. Pulmonary nodule detection in volumetric chest CT scans using CNNs-based nodule-size-adaptive detection and classification. *IEEE Access* 2019; 7: 46033-44.
  96. Wang C, Chen D, Hao L, et al. Pulmonary image classification based on inception-v3 transfer learning model. *IEEE Access* 2019; 7: 146533-41.
  97. Liu Y, Hao P, Zhang P, et al. Dense convolutional binary-tree networks for lung nodule classification. *IEEE Access* 2018; 6: 49080-88.
  98. Li L, Liu Z, Huang H, et al. Evaluating the performance of a deep learning-based computer-aided diagnosis (DL-CAD) system for detecting and characterizing lung nodules: comparison with the performance of double reading by radiologists. *Thorac Cancer* 2019; 10: 183-92.
  99. Jin H, Li Z, Tong R, et al. A deep 3D residual CNN for false-positive reduction in pulmonary nodule detection. *Med Phys* 2018; 45: 2097-107.
  100. Teramoto A, Tsukamoto T, Kiriya Y, et al. Automated classification of lung cancer types from cytological images using deep convolutional neural networks. *Biomed Res Int* 2017; 2017: 4067832.
  101. Dou Q, Chen H, Yu L, et al. Multilevel contextual 3-D CNNs for false positive reduction in pulmonary nodule detection. *IEEE Trans Biomed Eng* 2016; 64: 1558-67.
  102. Wang S, Shi J, Ye Z, et al. Predicting EGFR mutation status in lung adenocarcinoma on computed tomography image using deep learning. *Eur Respir J* 2019; 53: 1800986.
  103. Wang C, Shao J, Lv J, et al. Deep learning for predicting subtype classification and survival of lung adenocarcinoma on computed tomography. *Transl Oncol* 2021; 14: 101141.
  104. Ardila D, Kiraly AP, Bharadwaj S, et al. End-to-end lung cancer screening with three-dimensional deep learning on low-dose chest computed tomography. *Nat Med* 2019; 25: 954-61.
  105. Shao J, Wang G, Yi L, et al. Deep learning empowers lung cancer screening based on mobile low-dose computed tomography in resource-constrained sites. *Front Biosci (Landmark Ed)* 2022; 27: 212.
  106. Wang C, Xu X, Shao J, et al. Deep learning to predict EGFR mutation and PD-L1 expression status in non-small-cell lung cancer on computed tomography images. *J Oncol* 2021; 2021: 5499385.
  107. Li R, Xiao C, Huang Y, et al. Deep learning applications in computed tomography images for pulmonary nodule detection and diagnosis: a review. *Diagnostics* 2022; 12: 298.
  108. Lakshmanaprabu SK, Mohanty SN, Shankar K, et al. Optimal deep learning model for classification of lung cancer on CT images. *Future Gener Comput Syst* 2019; 92: 374-82.
  109. Lee SM, Seo JB, Yun J, et al. Deep learning applications in chest radiography and computed tomography: current state of the art. *J Thorac Imaging* 2019; 34: 75-85.
  110. Bhatia S, Sinha Y, Goel L. Lung cancer detection: a deep learning approach. In: *Soft Comput for Problem Solving: SocProS 2017, Vol 2*. Singapore: Springer Singapore; 2018: 699-705.
  111. Tian P, He B, Mu W, et al. Assessing PD-L1 expression in non-small cell lung cancer and predicting responses to immune checkpoint inhibitors using deep learning on computed tomography images. *Theranostics* 2021; 11: 2098.
  112. Hu D, Zhang H, Li S, et al. Automatic extraction of lung cancer staging information from computed tomography reports: deep learning approach. *JMIR Med Inform* 2021; 9: e27955.
  113. Ashraf SF, Yin K, Meng CX, et al. Predicting benign, preinvasive, and invasive lung nodules on computed tomography scans using machine learning. *J Thorac Cardiovasc Surg* 2022; 163: 1496-505.
  114. Subramanian RR, Mourya RN, Reddy VPT, et al. Lung cancer prediction using deep learning framework. *Int J Control Autom* 2020; 13: 154-60.
  115. Rajasekar V, Vaishnav MP, Premkumar S, et al. Lung cancer disease prediction with CT scan and histopathological images feature analysis using deep learning techniques. *Results Eng* 2023; 18: 101111.
  116. Wankhade S, Vigneshwari S. A novel hybrid deep learning method for early detection of lung cancer using neural networks. *Healthc Anal* 2023; 3: 100195.
  117. Abunajm S, Elsayed N, ElSayed Z, et al. Deep learning approach for early stage lung cancer detection. *arXiv* 2023; arXiv:2302.02456.
  118. Avanzo M, Stancanello J, Pirrone G, et al. Radiomics and deep learning in lung cancer. *Strahlenther Onkol* 2020; 196: 879-87.
  119. Chao H, Shan H, Homayounieh F, et al. Deep learning predicts cardiovascular disease risks from lung cancer screening low dose computed tomography. *Nat Commun*. 2021; 12: 2963.
  120. Shakeel PM, Burhanuddin MA, Desa MI. Lung cancer detection from CT image using improved profuse clustering and deep learning instantaneously trained neural networks. *Meas* 2019; 145: 702-12.
  121. Zhang Q, Wang H, Yoon SW, et al. Lung nodule diagnosis on 3D computed tomography images using deep convolutional neural networks. *Procedia Manuf* 2019; 39: 363-70.
  122. Zhao L, Qian J, Tian F, et al. A weighted discriminative extreme learning machine design for lung cancer detection by an electronic nose system. *IEEE Trans Instrum Meas* 2021; 70: 1-9.
  123. Chen L, Liu K, Shen H, et al. Multimodality attention-guided 3-D detection of nonsmall cell lung cancer in 18 F-FDG PET/CT images. *IEEE Trans Radiat Plasma Med Sci* 2021; 6: 421-32.
  124. Gindi A, Al Attiatalla TA, Sami MM. A comparative study for comparing two feature extraction methods and two classifiers in classification of early-stage lung cancer diagnosis of chest x-ray images. *J Am Sci* 2014; 10: 13-22.
  125. Suzuki K, Kusumoto M, Watanabe SI, et al. Radiologic classification of small adenocarcinoma of the lung: radiologic-pathologic correlation and its prognostic impact. *Ann Thorac Surg* 2006; 81: 413-9.

126. Wang H, Guo XH, Jia ZW, et al. Multilevel binomial logistic prediction model for malignant pulmonary nodules based on texture features of CT image. *Eur J Radiol* 2010; 74: 124-9.
127. Horeweg N, Scholten ET, de Jong PA, et al. Detection of lung cancer through low-dose CT screening (NELSON): a prespecified analysis of screening test performance and interval cancers. *Lancet Oncol* 2014; 15: 1342-50.
128. Gartman EJ, Jankowich MD, Baptiste J, et al. Providence VA lung cancer screening program: performance: comparison of local false positive and invasive procedure rates to published trial data. In: *Clin strategies to improve lung cancer early detection: who is at risk here?* *Am Thoracic Soci* 2018; A2477.
129. Robbins SL, Kumar V, Abbas AK, et al. *Robbins and Cotran Pathologic Basis of Disease*. 8th ed. 2010.
130. Travis WD. Update on small cell carcinoma and its differentiation from squamous cell carcinoma and other non-small cell carcinomas. *Mod Pathol* 2012; 25: S18-30.
131. Chan BA, Coward JJ. Chemotherapy advances in small-cell lung cancer. *J Thorac Dis* 2013; 5 (Suppl 5): S565.
132. Sagawa M, Nakayama T, Tsukada H, et al. The efficacy of lung cancer screening conducted in 1990s: four case-control studies in Japan. *Lung Cancer* 2003; 41: 29-36.
133. Fontana R. Lung cancer screening: the Mayo Program. *J Occup Med* 1986; 28: 46-50.
134. Kubik A, Parkin DM, Khat M, et al. Lack of benefit from semi-annual screening for cancer of the lung: follow-up report of a randomized controlled trial on a population of high-risk males in Czechoslovakia. *Int J Cancer* 1990; 45: 26-33.
135. Raghunath VK, Zhao W, Pu J, et al. Feasibility of lung cancer prediction from low-dose CT scan and smoking factors using causal models. *Thorax* 2019; 74: 643-9.
136. Risse EK, Vooijs GP, Van't Hof MA. Relationship between the cellular composition of sputum and the cytologic diagnosis of lung cancer. *Acta Cytol* 1987; 31: 170-6.
137. MacDougall B, Weinerman B. The value of sputum cytology. *J Gen Intern Med* 1992; 7: 11-3.
138. Kennedy TC, Hirsch FR, Miller YE, et al. A randomized study of fluorescence bronchoscopy versus white-light bronchoscopy for early detection of lung cancer in high-risk patients. *Lung Cancer* 2000; 29: 244-5.
139. Toyoda Y, Nakayama T, Kusunoki Y, et al. Sensitivity and specificity of lung cancer screening using chest low-dose computed tomography. *Br J Cancer* 2008; 98: 1602-7.
140. Hinton G. Deep learning – a technology with the potential to transform health care. *JAMA* 2018; 320: 1101-2.
141. LeCun Y, Bengio Y, Hinton G. Deep learning. *Nature* 2015; 521: 436-44.
142. Ueda D, Shimazaki A, Miki Y. Technical and clinical overview of deep learning in radiology. *Jpn J Radiol* 2019; 37: 15-33.
143. Nam JG, Park S, Hwang EJ, et al. Development and validation of deep learning-based automatic detection algorithm for malignant pulmonary nodules on chest radiographs. *Radiology* 2019; 290: 218-28.
144. Manser R, Lethaby A, Irving LB, et al. Screening for lung cancer. *Cochrane Database Syst Rev* 2013; 2013: CD001991.
145. Berlin L. Radiologic errors, past, present and future. *Diagnosis* 2014; 1: 79-84.
146. Schwartz LH, Litière S, De Vries E, et al. RECIST 1.1 – update and clarification: from the RECIST committee. *Eur J Cancer* 2016; 62: 132-7.
147. Schwyzler M, Ferraro DA, Muehlethaler UJ, et al. Automated detection of lung cancer at ultralow dose PET/CT by deep neural networks – initial results. *Lung Cancer* 2018; 126: 170-3.
148. Sun W, Zheng B, Qian W. Automatic feature learning using multichannel ROI based on deep structured algorithms for computerized lung cancer diagnosis. *Comput Biol Med* 2017; 89: 530-9.
149. Hosny A, Parmar C, Coroller TP, et al. Deep learning for lung cancer prognostication: a retrospective multi-cohort radiomics study. *PLoS Med* 2018; 15: e1002711.
150. Tiwari L, Raja R, Awasthi V, et al. Detection of lung nodule and cancer using novel Mask-3 FCM and TWEDLNN algorithms. *Meas* 2021; 172: 108882.
151. Wu B, Zhou Z, Wang J, et al. Joint learning for pulmonary nodule segmentation, attributes and malignancy prediction. In: *IEEE 15th Int Symp Biomed Imaging (ISBI 2018)*. 2018: 1109-13.
152. Liu H, Cao H, Song E, et al. Multi-model ensemble learning architecture based on 3D CNN for lung nodule malignancy suspiciousness classification. *J Digit Imaging* 2020; 33: 1242-56.
153. Li J, Tao Y, Cai T. Predicting lung cancers using epidemiological data: a generative-discriminative framework. *IEEE/CAA J Autom Sin* 2021; 8: 1067-78.
154. Xie Y, Zhang J, Xia Y. Semi-supervised adversarial model for benign-malignant lung nodule classification on chest CT. *Med Image Anal* 2019; 57: 237-48.
155. Abdani SR, Zulkifley MA, Shahrudin MI, et al. Computer-assisted pterygium screening system: a review. *Diagnostics (Basel)* 2022; 12: 639.
156. Zulkifley MA, Moubark AM, Saputro AH, et al. Automated apple recognition system using semantic segmentation networks with group and shuffle operators. *Agriculture* 2022; 12: 756.
157. Stofa MM, Zulkifley MA, Zainuri MA. Skin lesions classification and segmentation: a review. *Int J Adv Comput Sci Appl* 2021; 12: 532-41.
158. Stofa MM, Zulkifley MA, Zainuri MA, et al. U-net with atrous spatial pyramid pooling for skin lesion segmentation. In *Proceedings of the 6th International Conference on Electrical, Control and Computer Engineering: InECCE2021, Kuantan, Pahang, Malaysia, 23rd August. 2022*. Springer.
159. Xu M, Qi S, Yue Y, et al. Segmentation of lung parenchyma in CT images using CNN trained with the clustering algorithm generated dataset. *Biomed Engineering Online* 2019; 18: 1-21.
160. Liu C, Pang M. Automatic lung segmentation based on image decomposition and wavelet transform. *Biomed Signal Process Control* 2020; 61: 102032.
161. Khanna A, Londhe ND, Gupta S, et al. A deep residual U-Net convolutional neural network for automated lung segmentation in computed tomography images. *Biocybern Biomed Eng* 2020; 40: 1314-27.
162. Comelli A, Coronello C, Dahiya N, et al. Lung segmentation on high-resolution computerized tomography images using deep learning: a preliminary step for radiomics studies. *J Imaging* 2020; 6: 125.
163. Ait Skourt B, El Hassani A, Majda A. Lung CT image segmentation using deep neural networks. *Procedia Comput Sci* 2018; 127: 109-13.
164. Hu Q, Souza LFD, Holanda GB, et al. An effective approach for CT lung segmentation using mask region-based convolutional neural networks. *Artif Intell Med* 2020; 103: 101792.

165. Setio AAA, Ciompi F, Litjens G, et al. Pulmonary nodule detection in CT images: false positive reduction using multi-view convolutional networks. *IEEE Trans Med Imaging* 2016; 35: 1160-9.
166. Negahdar M, Beymer D, Syeda-Mahmood T. Automated volumetric lung segmentation of thoracic CT images using fully convolutional neural network. In: *Med Imaging 2018: Comput-Aid Diagn.* 2018; 10575: 356-61.
167. Roy R, Chakraborti T, Chowdhury AS. A deep learning-shape driven level set synergism for pulmonary nodule segmentation. *Pattern Recogn Lett* 2019; 123: 31-8.